



# A Photonic Crystal Protein Hydrogel Sensor for *Candida albicans*

Zhongyu Cai, Daniel H. Kwak, David Punihaole, Zhenmin Hong, Sachin S. Velankar, Xinyu Liu,\* and Sanford A. Asher\*

**Abstract:** We report two-dimensional (2D) photonic crystal (PC) sensing materials that selectively detect *Candida albicans* (*C. albicans*). These sensors utilize Concanavalin A (Con A) protein hydrogels with a 2D PC embedded on the Con A protein hydrogel surface, that multivalently and selectively bind to mannan on the *C. albicans* cell surface to form crosslinks. The resulting crosslinks shrink the Con A protein hydrogel, reduce the 2D PC particle spacing, and blue-shift the light diffracted from the PC. The diffraction shifts can be visually monitored, measured with a spectrometer, or determined from the Debye diffraction ring diameter. Our unoptimized hydrogel sensor has a detection limit of around 32 CFU/mL for *C. albicans*. This sensor distinguishes between *C. albicans* and those microbes devoid of cell-surface mannan such as the gram-negative bacterium *E. coli*. This sensor provides a proof-of-concept for utilizing recognition between lectins and microbial cell surface carbohydrates to detect microorganisms in aqueous environments.

**B**acteria, fungi, and viruses are major causes of infectious diseases.<sup>[1]</sup> *Candida albicans* (*C. albicans*), for instance, is a disease-causing microbe found in the mouth, gut, and vagina of 40–80% of normal humans. Overgrowth of *C. albicans* causes systemic infections such as pneumonia, septicaemia, or endocarditis, especially in immunodeficient patients.<sup>[2]</sup> It is important to develop methods to detect these types of microbes in order to treat early-stage infections.<sup>[2d,3]</sup>

Conventional approaches for identifying pathogens in aquatic environments and fluid samples are based on filtration culture,<sup>[4]</sup> fluorescence<sup>[5]</sup> and DNA microarray methods.<sup>[6]</sup> These techniques, however, either are slow, semi-quantitative, or suffer from lack of specificity and sensitivity. Immunological and molecular biology approaches have recently been used to detect pathogen microbes with high sensitivity and selectivity. These methods include radioimmunoassays, enzyme-linked immunosorbent assays, and the polymerase chain reaction (PCR),<sup>[7]</sup> and use radioisotopes, enzymes, and DNA fragments respectively, to label antibodies or prepare PCR antibody arrays for microbial

pathogen detection. However, these methods are complex, time-consuming, and demand well-trained personnel. Simple, highly efficient, and label-free methods are imperative to identify microbes in different environments.

Recently, label-free photonic crystal (PC) approaches, especially porous silicon (Si) photonic crystals (PCs), have been used for the detection of microbes.<sup>[8]</sup> The Si PCs method utilizes “trap and track” mechanism to capture bacteria in the pores of Si PCs; the bacteria concentration is determined with high sensitivity through monitoring the intensity of the reflection spectra upon capture of bacteria. However, this method lacks specificity.<sup>[8a,b]</sup> A PC-copolymer-film-based immunochip has been developed to detect gram-negative bacteria with a 200 CFU/mL detection limit. However, the fabrication of this sensor is complicated and its stability is problematic because of the attachment of multiple antibodies to the 2D PC nanopillars.<sup>[8c]</sup>

Multivalent interactions between host-cell surface carbohydrates and microbial surface proteins are currently attracting intense interest for their potential sensing applications.<sup>[9]</sup> Novel sensors utilizing the carbohydrate–pathogen interactions have been developed to detect bacteria, such as *Escherichia coli* (*E. coli*).<sup>[10]</sup> Nevertheless, such approaches generally lack specificity, as host-cell surface carbohydrate diversity is limited, and many microbes express proteins that recognize the same set of host carbohydrates, such as, the cross-reactivity of type 1 fimbriae expressed by *Salmonella enterica* and *E. coli* toward mannose.<sup>[10a,11]</sup> An alternative approach that reverses this process would utilize proteins as the sensing motif to recognize microbial cell-surface carbohydrate structures. This method would be more general and specific, as microbial cell-surface carbohydrate structures are diverse and generally species-specific, and proteins in the form of anticarbohydrate antibodies<sup>[12]</sup> or lectins against specific microbial cell surface carbohydrate molecules<sup>[9b]</sup> can be readily obtained.

Herein we report multivalent protein–carbohydrate specific recognition with a PC optical readout methodology as a proof-of-principle study to demonstrate a new sensing motif. This sensor utilizes a carbohydrate-binding protein (lectin) to detect *C. albicans*, a major nosocomial fungal pathogen, selectively from those microbial organisms that lack cell-surface mannan units, such as gram-negative bacterium *E. coli*. Mannans are the major surface carbohydrates in *C. albicans* and play important roles in cell-wall integrity, adhesion to host cells and tissues, and virulence.<sup>[13]</sup> We show that the specific recognition between the lectin Concanavalin A (Con A) and mannan can be used to detect the presence of *C. albicans*. The pure Con A protein hydrogels are fabricated by crosslinking Con A solutions with glutaraldehyde. A 2D PC array of monodisperse particles is attached to the

[\*] Dr. Z. Cai, D. H. Kwak, D. Punihaole, Dr. Z. Hong, Prof. X. Liu, Prof. S. A. Asher  
Department of Chemistry, University of Pittsburgh  
Pittsburgh, PA 15260 (USA)  
E-mail: xinyuliu@pitt.edu  
asher@pitt.edu

Prof. S. S. Velankar  
Department of Chemical Engineering, University of Pittsburgh  
Pittsburgh, PA 15261 (USA)

Supporting information for this article is available on the WWW under <http://dx.doi.org/10.1002/anie.201506205>.

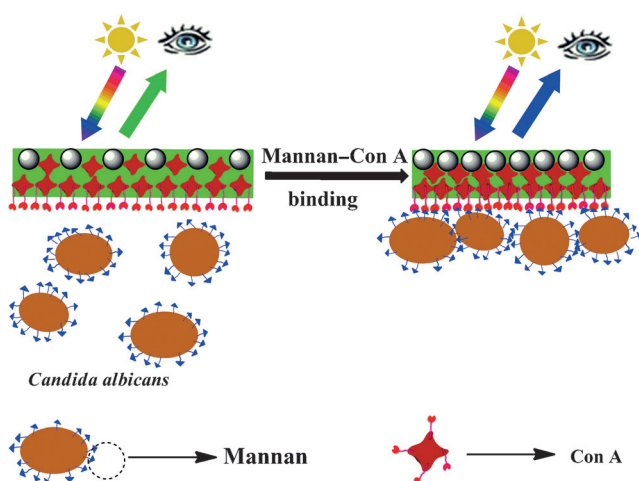


**Figure 1.** Schematic illustration of Con A–*C. albicans* mannan binding. The detailed structure of mannan and Con A can be found in Figure S2. Figure is not to scale, approximate dimensions: Con A hydrogel thickness: 100  $\mu\text{m}$ , *C. albicans* diameter: 5  $\mu\text{m}$ , PS spheres diameter: 0.65  $\mu\text{m}$ .

hydrogel surface, and the diffraction from the array is related to the hydrogel volume. The hydrogel Con A proteins each bind multiple mannose groups to surface-crosslink the protein hydrogel and result in shrinking and a decrease in the 2D array particle spacing (Figure 1). The decrease in particle spacing results in a blue-shift of the 2D array diffraction, which reports on the *C. albicans* concentration. Compared to previous methods, our method is simple, more selective, highly efficient and inexpensive.

We fabricated the 2D PC arrays using monodisperse polystyrene (PS) spheres (ca. 650 nm in diameter) that were synthesized by emulsion polymerization.<sup>[14]</sup> The needle tip flow technique was used to self-assemble the PS spheres into a close-packed 2D PC array on a water surface.<sup>[15]</sup> The 2D PCs were then transferred onto a glass slide and dried in air. The Con A protein hydrogel was prepared by mild crosslinking of a Con A monomer solution with glutaraldehyde on top of the 2D PCs.<sup>[16]</sup> The 2D PC–Con A hydrogels were peeled off the glass slides and equilibrated with phosphate buffer at pH 9. The resulting PC hydrogels, which were approximately 100  $\mu\text{m}$  thick, show iridescent colors under white-light illumination as a result of the 2D array diffraction (Figure 2a).

These PC–Con A hydrogels swell upon washing and equilibration in buffer such that the 2D array becomes non-close-packed (Figure 2a (inset) and Figure S3 in the Supporting Information). The 2D array diffraction sensitively reports on the hydrogel volume. We typically monitor the array spacing by measuring the 2D array Debye ring diameter as discussed in the Supporting Information (Figure S1).

The PC–Con A hydrogels consist of essentially native-conformation Con A proteins as indicated by UV resonance Raman spectroscopy (Figure S4). The secondary structure of the Con A protein crosslinked in the hydrogel is essentially identical to that of the native Con A monomer in solution.

Con A binds mannose monomers as well as mannose polymers, such as mannan isolated from yeast cell walls. The

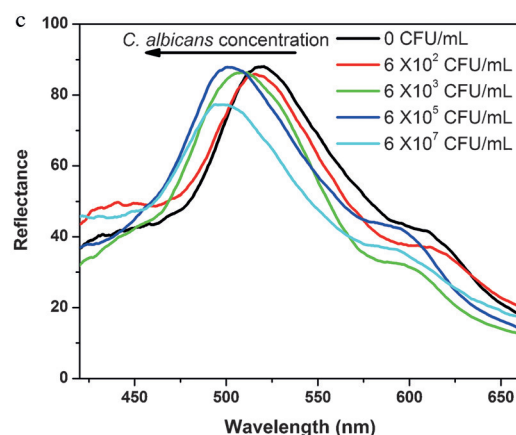
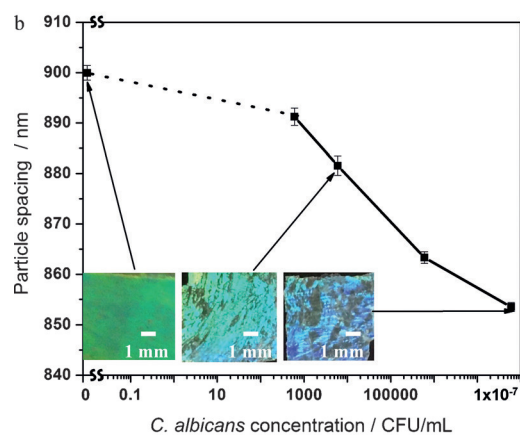
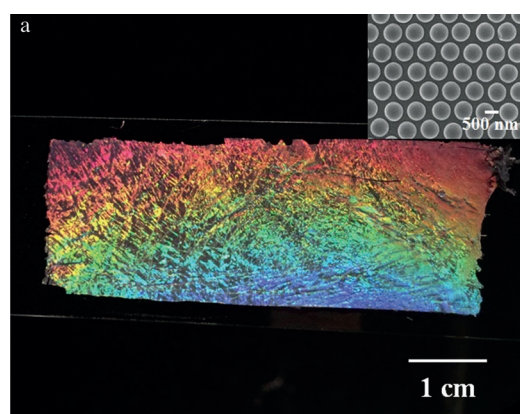


**Figure 2.** a) Photograph of Con A protein hydrogel crosslinked by glutaraldehyde illuminated with a flashlight below at an angle of around 40° from the normal. The diffraction of the white light gives rise to iridescence. The inset SEM image shows the non-close-packed 2D PC embedded on the Con A hydrogel. b) *C. albicans* concentration dependence of PC–Con A hydrogel particle spacing. The photographs show the color of the forward-diffracted light taken with a camera along the normal and the source below at an angle of around 70.5° to the 2D array normal. c) *C. albicans* concentration dependence of the hydrogel sensor reflectance measured with a spectrometer in the Littrow configuration, which is that where the diffracted light diffracts back parallel to the direction of the incident light.

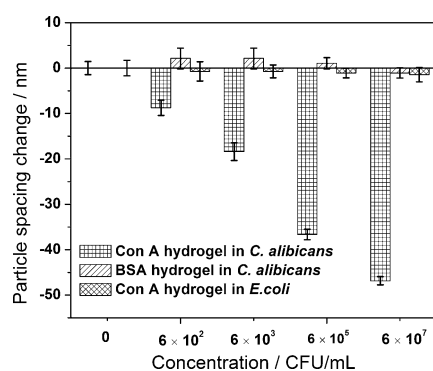
titration of the hydrogel sensor with mannose up to 5 mg mL<sup>−1</sup> results in a small (<20 nm) concentration-dependent decrease in the particle spacing (Figure S5). The Con A–

mannose binding probably reduces the favorability of the free energy of mixing of the resulting hydrogel, which leads to a modest Con A hydrogel shrinkage. In contrast, a large (ca. 70 nm) particle spacing decrease results from Con A-mannan multidentate binding,<sup>[17]</sup> which forms crosslinks that shrink the Con A hydrogel.<sup>[11,18]</sup> The Con A-mannan recognition mechanism is discussed in the Supporting Information (Figure S6).<sup>[18]</sup>

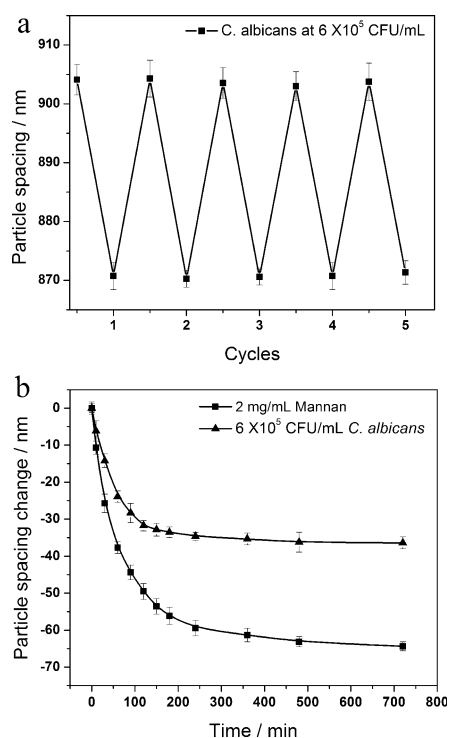
This Con A-mannan binding can be used to sense the presence of *C. albicans* because of the presence of its surface mannan units. Figure 2b shows the *C. albicans* concentration dependence of the PC-Con A hydrogel particle spacing. The particle spacing decreases with increasing *C. albicans* concentration. An 8 nm particle spacing decrease occurs upon introduction of the sensor to 20 mL *C. albicans* at an initial concentration of  $6 \times 10^2$  CFU/mL (the free concentration of *C. albicans* is estimated to be ca. 60 CFU/mL). A larger 47 nm particle spacing decrease occurs upon incubation in a 20 mL *C. albicans* solution at an initial concentration of around  $6 \times 10^7$  CFU/mL. We calculated the limit of detection (LoD) for this unoptimized PC-Con A hydrogel to be around 32 CFU/mL (see the Supporting Information for details of the calculation), which is much lower than the physiologically typical concentration (400 CFU/mL in saliva).<sup>[19]</sup> The binding of *C. albicans* to the PC-Con A hydrogel shifts the visually observed diffracted color from green to blue (Figure 2b inset), which is consistent with the diffraction wavelength maximum measured by using a reflection probe in the Littrow configuration at an angle of  $19.5^\circ$  between the probe and the 2D array normal. In a Littrow configuration, the 2D Bragg diffraction relationship is  $m\lambda = 3^{1/2}d \sin \theta$ , where  $m$  is the diffraction order,  $\lambda$  is the diffracted wavelength (in vacuum),  $d$  is the 2D particle spacing, and  $\theta$  is the angle of the light relative to the normal to the 2D array.<sup>[20]</sup> As shown in Figure 2c and Figure S7, the diffraction maximum shifts from 521 to 493 nm, which matches the particle spacing change (from 900 to 853 nm) measured from the Debye diffraction diameter.<sup>[20]</sup>

Figure S8 shows optical micrographs of Con A hydrogel surfaces incubated at different *C. albicans* concentrations. At an initial concentration of approximately  $6 \times 10^2$  CFU/mL, the free Con A hydrogel surface shows sparse *C. albicans* binding, whereas this surface is highly bound at around  $6 \times 10^5$  CFU/mL. Figure S8d shows that *C. albicans* binds negligibly to the surface of the Con A hydrogel attached to the 2D PS arrays. *C. albicans* cells are approximately 5–8  $\mu\text{m}$  in diameter,<sup>[21]</sup> which greatly exceeds the interstice size of the 2D array. Therefore, *C. albicans* cannot penetrate into the Con A protein hydrogel.

The PC-Con A sensor selectively detects *C. albicans*, as evident by the particle-spacing change of the 2D PC on the Con A hydrogel. As can be seen in Figure 3, a particle-spacing decrease of around 47 nm occurs upon the Con A hydrogel exposure to  $6 \times 10^7$  CFU/mL *C. albicans*. This large decrease arises from the relatively strong multivalent binding of the *C. albicans* mannan to the hydrogel Con A to form crosslinks. It is reported that the Con A equilibrium association constant for mannan is  $3.46 \times 10^5 \text{ m}^{-1}$ .<sup>[22]</sup> In contrast, the Con A sensor does not respond to *E. coli*, thus indicating that no significant



**Figure 3.** *C. albicans* concentration dependence of the particle spacing change of the PC-Con A and PC-BSA hydrogels. Also shown is the *E. coli* concentration dependence of the PC-Con A protein hydrogel particle spacing change.



**Figure 4.** a) Reversibility of PC-Con A hydrogel particle spacing changes to *C. albicans* initial concentrations of  $6 \times 10^5$  CFU/mL. b) Time dependence of particle spacings in response to saturating concentrations of *C. albicans* ( $6 \times 10^5$  CFU/mL) and mannan ( $2 \text{ mg mL}^{-1}$ ).

binding between the Con A hydrogel and *E. coli* occurs because of the lack of mannan on its surface.<sup>[1b,23]</sup> It was also found that there is little particle-spacing change (ca. 2 nm) for a BSA protein hydrogel upon exposure to  $6 \times 10^7$  CFU/mL *C. albicans*, because *C. albicans* surface mannan does not bind to BSA. An SEM measurement of the BSA protein hydrogel surface confirms the lack of *C. albicans* binding (Figure S10).

We investigated the reversibility of the PC-Con A sensor's response to *C. albicans*. Repeated exposure to  $6 \times 10^5$  CFU/mL *C. albicans* followed by washing with phosphate buffer demonstrates the reversibility of the sensor. Figure 4a

shows that our PC–Con A hydrogel is completely reversible over five cycles toward *C. albicans* in solution.

The kinetics of the response of our PC–Con A hydrogel sensor to *C. albicans* and mannan is shown in Figure 4b. The saturating mannan concentration ( $2 \text{ mg mL}^{-1}$ ; Figure S5) gives twice the shrinkage of the Con A hydrogel, as does a saturating *C. albicans* solution ( $6 \times 10^5 \text{ CFU/mL}$ ). This large shrinkage presumably results from the better ability of mannan to penetrate into the Con A hydrogel. Under gentle agitation, binding of both *C. albicans* and mannan to the Con A hydrogel saturates within around 100 min. The similar response kinetics argues for a sensing mechanism that is limited by the hydrogel response time, and may be due to the slow diffusion of *C. albicans* and mannan molecules into the Con A hydrogel.<sup>[22,24]</sup> The mannan has a large molecular weight of 54 kDa as determined by using SEC/GPC, which also makes it difficult to fully diffuse into the Con A.<sup>[22]</sup>

In summary, we developed 2D PC–Con A hydrogel sensing materials for the detection of the fungal pathogen *C. albicans*. The cell-surface mannan binding to hydrogel Con A sites form crosslinks, which shrink the Con A hydrogel volume and decrease the 2D array particle spacing, to result in visually evident blue-shifts of the diffracted light, and an increase in the Debye ring diameter. The reported PC–Con A hydrogel selectively senses *C. albicans* over *E. coli* bacteria with a significantly shortened detection time from around 2 d by filtration culture methods<sup>[4]</sup> to less than 2 h at a low LoD of 32 CFU/mL. While this sensor, which utilizes Con A as the sensing motif, cannot distinguish *C. albicans* from other microbes that also express cell-surface mannan (e.g., *S. cerevisiae*, Figure S11),<sup>[25]</sup> it demonstrates that the combination of a 2D PC platform with a carbohydrate-binding protein hydrogel is an effective approach for developing sensors for microbial detection. Antibodies against specific cell-surface carbohydrate antigens can be raised and obtained rapidly,<sup>[12a]</sup> and therefore are expected to be quickly incorporated into this platform to achieve absolute selectivity. Furthermore, by optimizing the responsivity and detection time, this approach may find a wide variety of applications in sensing biological, chemical, and clinical agents in potential terrorism threats, healthcare, and disease diagnosis.<sup>[26]</sup> Currently, we are working on the fabrication of less crosslinked, thinner hydrogels in order to further improve the sensitivity and to decrease the detection times of these PC–Con A sensors.

## Acknowledgements

We gratefully acknowledge HDTRA (grant no. 1-10-1-0044 to SAA), the Department of Chemistry, University of Pittsburgh (startup fund to X.L.), and NSF-CBET-1336311 to SV for funding.

**Keywords:** gels · microbes · photonic crystals · proteins · sensors

**How to cite:** *Angew. Chem. Int. Ed.* **2015**, *54*, 13036–13040  
*Angew. Chem.* **2015**, *127*, 13228–13232

- [1] a) A. Varki, *Glycobiology* **1993**, *3*, 97–130; b) K. A. Karlsson, *Biochem. Soc. Trans.* **1999**, *27*, 471–474.
- [2] a) <http://www.cdc.gov/fungal/diseases/candidiasis/>; b) L. de Repentigny, D. Lewandowski, P. Jolicoeur, *Clin. Microbiol. Rev.* **2004**, *17*, 729–759; c) D. MacCallum in *Pathogenic Yeasts* (Eds.: R. Ashbee, E. M. Bignell), Springer, Berlin, **2010**, pp. 41–67; d) R. A. Calderone, W. A. Fonzi, *Trends Microbiol.* **2001**, *9*, 327–335.
- [3] “Bacterial and Viral Infections”: V. Nizet, J. D. Esko in *Essentials of Glycobiology* (Eds: A. Varki, R. D. Cummings, J. D. Esko, H. H. Freeze, P. Stanley, C. R. Bertozzi, G. W. Hart, M. E. Etzler), Cold Spring Harbor Laboratory Press, New York, **2009**, chap. 39.
- [4] J. M. Jones, *Clin. Microbiol. Rev.* **1990**, *3*, 32–45.
- [5] a) A. Lischewski, R. I. Amann, D. Harmsen, H. Merkert, J. Hacker, J. Morschhäuser, *Microbiology* **1996**, *142*, 2731–2740; b) A. W. Lantz, B. Bisha, M.-Y. Tong, R. E. Nelson, B. F. Brehm-Stecher, D. W. Armstrong, *Electrophoresis* **2010**, *31*, 2849–2853.
- [6] a) D. M. Leinberger, U. Schumacher, I. B. Autenrieth, T. T. Bachmann, *J. Clin. Microbiol.* **2005**, *43*, 4943–4953; b) B. Spiess, W. Seifarth, M. Hummel, O. Frank, A. Fabarius, C. Zheng, H. Mörz, R. Hehlmann, D. Buchheidt, *J. Clin. Microbiol.* **2007**, *45*, 3743–3753.
- [7] a) S. Huang, C. Berry, J. Newman, W. Cooper, N. Zachariah, *Mycopathologia* **1979**, *67*, 55–58; b) W. M. Scheld, R. S. Brown, Jr., S. A. Harding, M. A. Sande, *J. Clin. Microbiol.* **1980**, *12*, 679–683; c) H. Xiang, L. Xiong, X. Liu, Z. Tu, *J. Microbiol. Methods* **2007**, *69*, 282–287; d) Y. Miyakawa, T. Mabuchi, Y. Fukazawa, *J. Clin. Microbiol.* **1993**, *31*, 3344–3347.
- [8] a) N. Massad-Ivanir, Y. Mirsky, A. Nahor, E. Edrei, L. M. Bonanno-Young, N. Ben Dov, A. Sa’ar, E. Segal, *Analyst* **2014**, *139*, 3885–3894; b) C.-C. Wu, S. D. Alvarez, C. U. Rang, L. Chao, M. J. Sailor, *Proc. SPIE* **2009**, *7167*, 71670Z; c) N. Li, X. R. Cheng, A. Brahmendra, A. Prashar, T. Endo, C. Guyard, M. Terebiznik, K. Kerman, *Biosens. Bioelectron.* **2013**, *41*, 354–358.
- [9] a) S. M. Borisov, O. S. Wolfbeis, *Chem. Rev.* **2008**, *108*, 423–461; b) R. Jelinek, S. Kolusheva, *Chem. Rev.* **2004**, *104*, 5987–6016.
- [10] a) M. D. Disney, J. Zheng, T. M. Swager, P. H. Seeberger, *J. Am. Chem. Soc.* **2004**, *126*, 13343–13346; b) Z. Shen, M. Huang, C. Xiao, Y. Zhang, X. Zeng, P. G. Wang, *Anal. Chem.* **2007**, *79*, 2312–2319.
- [11] M. Mammen, S.-K. Choi, G. M. Whitesides, *Angew. Chem. Int. Ed.* **1998**, *37*, 2754–2794; *Angew. Chem.* **1998**, *110*, 2908–2953.
- [12] a) R. D. Astronomo, D. R. Burton, *Nat. Rev. Drug Discovery* **2010**, *9*, 308–324; b) A. Weintraub, *Carbohydr. Res.* **2003**, *338*, 2539–2547.
- [13] R. A. Hall, N. A. R. Gow, *Mol. Microbiol.* **2013**, *90*, 1147–1161.
- [14] C. E. Reese, S. A. Asher, *J. Colloid Interface Sci.* **2002**, *248*, 41–46.
- [15] J.-T. Zhang, L. Wang, D. N. Lamont, S. S. Velankar, S. A. Asher, *Angew. Chem. Int. Ed.* **2012**, *51*, 6117–6120; *Angew. Chem.* **2012**, *124*, 6221–6224.
- [16] Z. Cai, J.-T. Zhang, F. Xue, Z. Hong, D. Punihale, S. A. Asher, *Anal. Chem.* **2014**, *86*, 4840–4847.
- [17] H. Lis, N. Sharon, *Chem. Rev.* **1998**, *98*, 637–674.
- [18] J.-T. Zhang, Z. Cai, D. H. Kwak, X. Liu, S. A. Asher, *Anal. Chem.* **2014**, *86*, 9036–9041.
- [19] J. B. Epstein, N. N. Pearsall, E. L. Truelove, *J. Clin. Microbiol.* **1980**, *12*, 475–476.
- [20] a) I. M. Krieger, F. M. O’Neill, *J. Am. Chem. Soc.* **1968**, *90*, 3114–3120; b) A. Tikhonov, N. Kornienko, J.-T. Zhang, L. Wang, S. A. Asher, *J. Nanophotonics* **2012**, *6*, 063509.
- [21] K. S. Kim, Y. S. Kim, I. Han, M. H. Kim, M. H. Jung, H. K. Park, *PLoS One* **2011**, *6*, e28176.
- [22] F. S. Coulibaly, B.-B. C. Youan, *Biosens. Bioelectron.* **2014**, *59*, 404–411.

- [23] K.-A. Karlsson in *The Molecular Immunology of Complex Carbohydrates—2, Vol. 491* (Ed.: A. Wu), Springer, New York, **2001**, pp. 431–443.
- [24] T. Mori, M. Toyoda, T. Ohtsuka, Y. Okahata, *Anal. Biochem.* **2009**, *395*, 211–216.
- [25] F. M. Klis, C. G. de Koster, S. Brul, *Eukaryotic Cell* **2014**, *13*, 2–9.
- [26] a) J. Ge, Y. Yin, *Angew. Chem. Int. Ed.* **2011**, *50*, 1492–1522; *Angew. Chem.* **2011**, *123*, 1530–1561; b) C. Fenzl, T. Hirsch, O. S. Wolfbeis, *Angew. Chem. Int. Ed.* **2014**, *53*, 3318–3335; *Angew. Chem.* **2014**, *126*, 3384–3402; c) Z. Cai, N. L. Smith, J.-T. Zhang, S. A. Asher, *Anal. Chem.* **2015**, *87*, 5013–5025.

Received: July 6, 2015

Published online: September 7, 2015